

Impacts of Optical Properties of Anti-Reflection Coatings on Characteristics of InGaP/GaAs/Si Hybrid Triple-Junction Cells

Naoteru Shigekawa and Jianbo Liang

Osaka City University, 3-3-138 Sugimoto, Sumiyoshi, Osaka 558-8585, Japan

Abstract—InGaP/GaAs/Si hybrid triple-junction cells with 95-nm SiN/65-nm SiO₂ bilayer and 75-nm SiN monolayer films as anti-reflection (AR) coatings were investigated. A more marked imbalance in photo currents of subcells was observed in cells with SiN monolayer films. The difference in imbalance was attributed to the optical properties of coatings. The short-circuit currents of the two triple-junction cells were close to each other and were larger than photo currents in the Si bottom cells while the open-circuit voltages were slightly different. These findings suggested that subcells might be electrically coupled to each other in multi-junction operations.

Index Terms—multi-junction cell, InGaP, GaAs, Si, surface activated bonding, spectral response, electrical coupling

I. INTRODUCTION

Multi-junction solar cells made of III-V semiconductors are promising as practical candidate for next-generation high-efficiency solar cells due to their high conversion efficiencies. Conversion efficiencies > 30% were reported for InGaP/InGaAs/Ge and InGaP/GaAs/InGaAs triple-junction cells [1], [2]. A conversion efficiency of 44.47% was achieved for InGaP/GaAs/InGaAsP/InGaAs four-junction cells [3]. Multi-junction cells with Si-based bottom cells are intensively investigated so as to simultaneously realize high efficiencies and low costs. The possibility of such cells has been examined by using both monolithic (crystal-growth based) [4] as well as hybrid (wafer-bonding based) approaches [5], [6].

It is assumed that the surface activated bonding (SAB) [7], [8] is an ideal method for fabricating multi-junction cells on Si since the dissimilar semiconductor materials can be bonded to each other without using any intermediate layers in low temperatures. Based on fundamental studies on SAB-based interfaces of dissimilar materials [9], [10], we fabricated InGaP/Si double-junction cells and observed the enhancement of open-circuit voltages (V_{OC}) [11]. We recently fabricated InGaP/GaAs/Si hybrid triple-junction cells by using SAB [12] and estimated the conversion efficiency for a $5 \times 5 \text{ mm}^2$ cell to be $\approx 23\%$ by subtracting the contribution of Si ledge. It was assumed that the result corresponded to an intrinsic conversion efficiency of $\approx 26\%$ based on the shadow loss estimation [13]. Here we note that InGaP/GaAs/Si stacks are not optimum from the viewpoint of bandgaps since the number of photons absorbed in the bottom cell is smaller than that of photons absorbed in the top or middle cells. It should also be noted that the numbers of photons absorbed in the respective subcells might be varied due to the reflectivity spectrum of employed anti-reflection (AR) coatings.

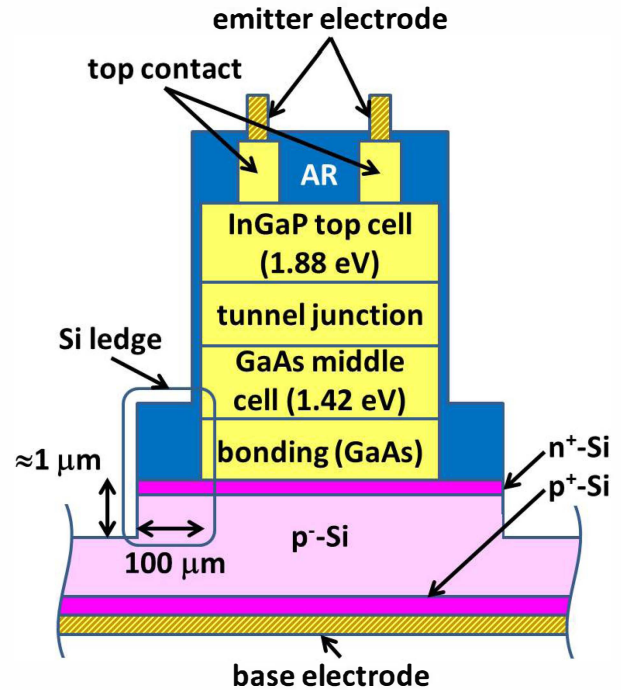


Fig. 1. A schematic cross section of InGaP/GaAs/Si triple-junction cells.

In this work, we fabricated InGaP/GaAs/Si hybrid triple-junction cells with SiN monolayer and SiN/SiO₂ bilayer films as AR coatings. We characterized their performances with emphasis on the correlation among the properties of AR coatings, the characteristics of respective subcells, and the characteristics in the multi-junction operation.

II. RESULTS AND DISCUSSION

A. Sample Preparation

We fabricated *n-on-p* InGaP/GaAs/Si triple-junction cells by (i) surface-activated bonding of MOVPE-grown InGaP/GaAs double-cell structures to Si-based bottom cell structures, (ii) selectively etching GaAs substrates, and (iii) employing conventional cell process sequences. The entire bonding process was performed without heating samples. The emitter in bottom cell structures had been prepared by the implantation of phosphor (P) ions to high-resistive *p*-type Si (100) substrates and the subsequent annealing (900 °C, 1 min.). A preparatory measurement indicated that the maximum concentration of

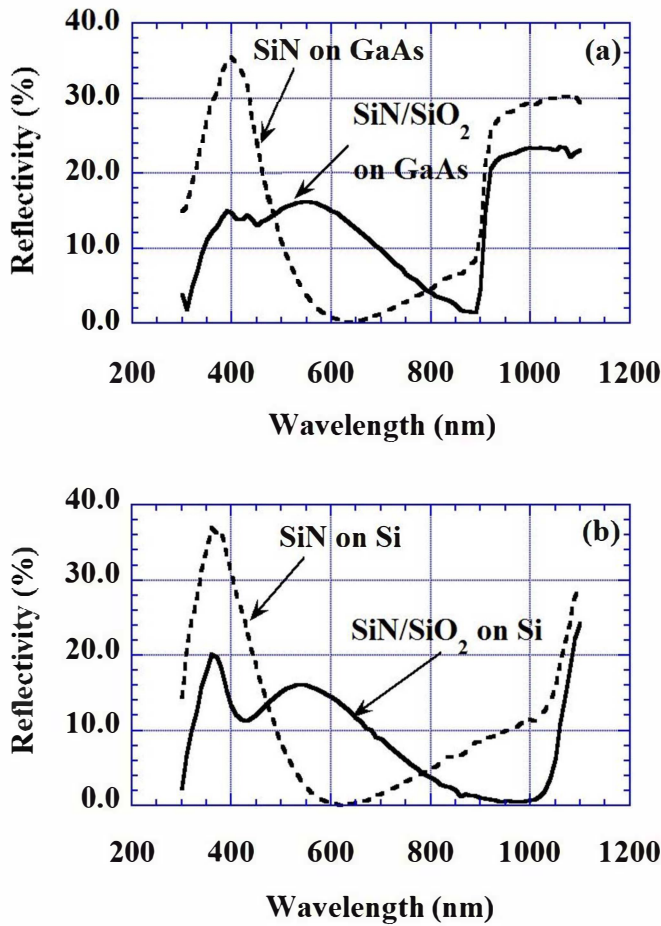


Fig. 2. Reflectivity spectra of SiN monolayer and SiN/SiO₂ bilayer films deposited on (a) a GaAs substrate and (b) a Si substrate.

P atoms in the emitter was as high as $\sim 6 \times 10^{19} \text{ cm}^{-3}$ at a depth of 10 nm. The employed semiconductor device process steps were composed of emitter electrode formation, top-contact-layer etching, III-V mesa etching, AR coating deposition, isolation etching of Si junction with a depth of $\approx 1 \mu\text{m}$, base electrode formation. Si ledges with an extension of 100 μm surrounding III-V mesa were inevitably made in the step of isolation etching of bottom cell junctions. 75-nm-thick SiN monolayers and 95-nm SiN/65-nm SiO₂ bilayers were employed as AR coatings. A schematic cross section of the triple-junction cells is shown in Fig. 1. The details of the entire fabrication process were previously reported [12], [13]. We also fabricated *n-on-p* single-junction Si cells with both types of films as AR coatings. Furthermore the two types of films were deposited on Si and GaAs substrates for optical characterization.

B. Characterization of AR Coatings and Cells

The optical reflectivity of the two types of films was measured between 300 and 1100 nm. The obtained spectra for films on Si and GaAs substrates are shown in Figs. 2(a) and (b), respectively. We find that the reflectivity of the SiN/SiO₂

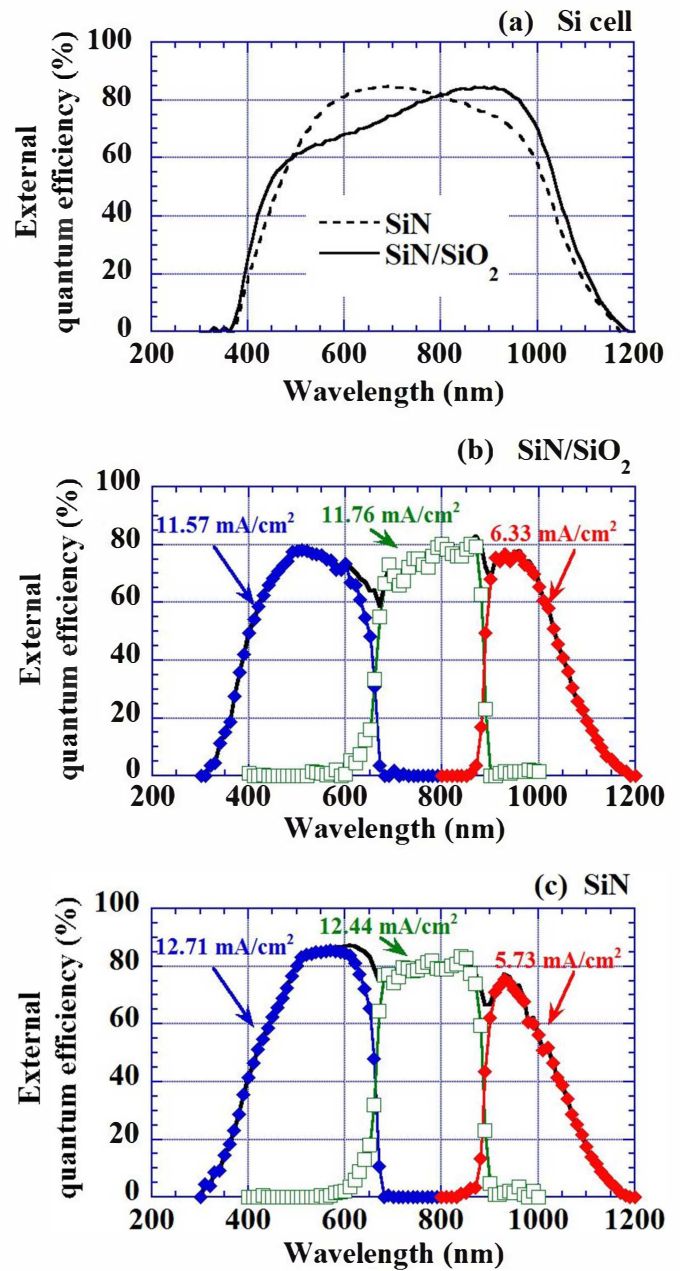


Fig. 3. EQE spectra of (a) $2 \times 2 \text{ mm}^2$ Si cells with two types of AR coatings, (b) a $2 \times 2 \text{ mm}^2$ InGaP/GaAs/Si triple-junction cell with a SiN/SiO₂ bilayer film as AR coating, and (c) a triple-junction cell with a SiN monolayer film as AR coating. Photo currents generated in the respective subcell under the AM1.5G and one sun condition are also shown in (b) and (c).

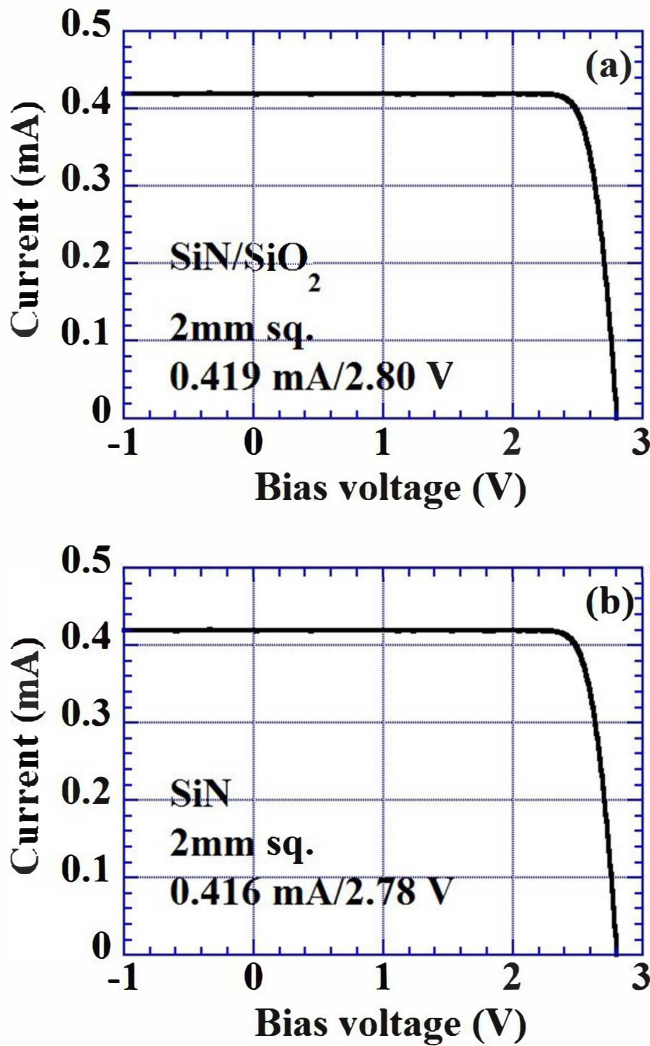


Fig. 4. As-measured current-voltage characteristics for the solar irradiance of air mass 1.5G and one sun of a $2 \times 2 \text{ mm}^2$ InGaP/GaAs/Si triple-junction cell (a) with a SiN/SiO₂ bilayer film as AR coating, and (b) with a SiN monolayer film as AR coating.

bilayer is lower than the reflectivity of the SiN monolayer for wavelengths $> 800 \text{ nm}$ on each substrate. We also measured spectral responses of $2 \times 2 \text{ mm}^2$ single-junction Si cells with the respective AR coatings. Their external quantum efficiency (EQE) spectra are compared in Fig. 3(a). The EQE of cells with SiN/SiO₂-based AR coatings is larger than that of cells with SiN-based AR coatings for wavelengths $> 800 \text{ nm}$, which is in accordance with the behavior in the reflectivity.

EQE spectra of $2 \times 2 \text{ mm}^2$ InGaP/GaAs/Si triple-junction cells with the two kinds of AR coatings are shown in Figs. 3(b) and (c), respectively. Photo currents generated in respective subcells under a solar irradiance of air mass 1.5G and one sun are also shown. As is shown in Fig. 3(b), the currents are estimated to be 11.57, 11.76, and 6.33 mA/cm² for the top, middle, and bottom cells of triple-junction cells with SiN/SiO₂ bilayers. In triple-junction cells with SiN monolayers, the

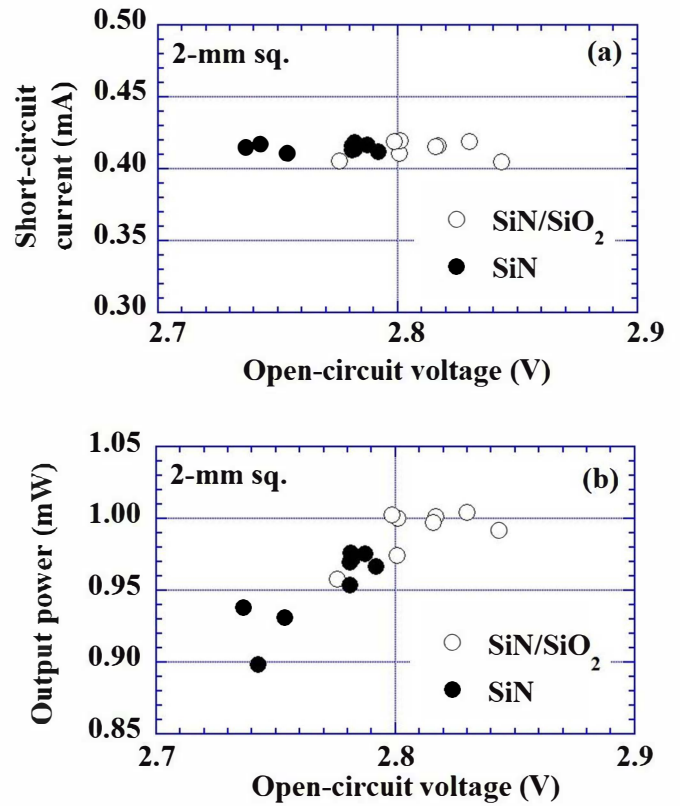


Fig. 5. Relationships (a) between the short-circuit current and V_{OC} and (b) between the output power and V_{OC} of triple-junction cells with two types of AR coatings. Contribution of Si ledges was not subtracted.

currents are 12.71 (top), 12.44 (middle), and 5.73 mA/cm² (bottom cell), as is seen from Fig. 3(c). The EQE signal of the bottom cell was more significant and its photo current was larger in triple-junction cells coated by SiN/SiO₂ films, which is consistent with the features of EQE spectra of single-junction Si cells. We also found that the imbalance in photo currents of subcells was more marked in triple-junction cells with SiN monolayer films.

The current-voltage characteristics of the two triple-junction cells were measured for the condition of air mass 1.5G and one sun. The as-measured characteristics are shown in Figs. 4(a) and (b), respectively. Their short-circuit currents were found to be 0.419 and 0.416 mA for cells with SiN/SiO₂ and SiN films, respectively. By subtracting the contribution of the Si ledge to the short-circuit current, whose magnitude per unit length of Si periphery is estimated to be $\approx 0.012 \text{ mA/mm}$, the intrinsic short-circuit current is assumed to be $\approx 0.32 \text{ mA}$ for both cells. The resultant short-circuit current density (J_{SC}) should be $\approx 8 \text{ mA/cm}^2$. It is noteworthy that the observed J_{SC} of each triple-junction cell is higher than the photo current density estimated for its bottom cell.

The relationship between the short-circuit current and V_{OC} and that between the output power and V_{OC} of the all $2 \times 2 \text{ mm}^2$ triple-junction cells with both types of AR films are shown in Figs. 5(a) and (b), respectively. The contribution of Si

ledges is not subtracted. We find V_{OC} of cells with SiN/SiO₂ bilayers is larger than that of cells with SiN monolayer films by ≈ 0.05 V whilst the short-circuit currents of the two types of cells almost agree with each other. The output power of the cells with SiN/SiO₂ bilayers is larger than that of cells with SiN monolayers due to the difference in V_{OC} .

C. Discussion: Possible Electrical Coupling between Subcells

The result that J_{SC} of each triple-junction cell is higher than the density of photo current in its bottom cell disagrees with a simple view that J_{SC} of multi-junction cells should be limited by the photo currents in the constituent subcells. The disagreement suggests that there occurs some kind of coupling between subcells in actual multi-junction cells. The present authors previously discussed a hypothetical process for explaining the disagreement that (i) the imbalance between photo currents in the respective subcells induced the pile-up of surplus holes in the p -doped base or the contact layer of the middle cells, (ii) the potential of this region is modulated due to the electrostatic effects, and (iii) the holes are injected toward the bottom cells beyond the lowered barriers between the p -doped base/contact layers of the middle cells and the n -doped emitter of the bottom cells [13]. Such a process could occur since the emitter of the bottom cells is several-nm thick and heavily doped, which suggests that the holes can easily be transferred from the contact layer of middle cells to the base of the bottom cells. Furthermore it is noteworthy that performances of photo transistors [14] as well as kink in current-voltage characteristics of InGaAs-based HEMTs [15] are analyzed using a similar picture, i.e., the electrostatic effects due to the pile-up of surplus carriers.

The observed difference in V_{OC} hence the difference in the conversion efficiency between the two types of triple-junction cells is likely to be explained by using such electrical-coupling scheme; The potential of the base or the contact layer of the middle cell in triple-junction cells with SiN monolayer AR films is more largely modulated so as to compensate for the larger imbalance in currents of subcells. Consequently, the tunnel junctions between the middle and bottom cells in triple-junction cells with SiN monolayer AR films are more markedly forward-biased so that their V_{OC} should be lowered. Anyhow the obtained results that J_{SC} in multi junction cells was intermediate among photo currents in the respective subcells suggest that the requirements for the current matching in multi junction cells could be relaxed.

III. CONCLUSION

InGaP/GaAs/Si hybrid triple-junction cells coated by a SiN monolayer and a SiN/SiO₂ bilayer were characterized. Their spectral response measurements showed that photo currents generated in the respective subcells are varied by changing the optical properties of AR coatings. The imbalance in photo currents was larger in triple-junction cells with SiN coatings. It was also found that J_{SC} in the multi junction operation was almost the same with each other and higher than the estimated photo current density of the Si bottom cells. The difference

between J_{SC} and the photo current density in the Si bottom cell as well as the difference in V_{OC} between the two types of triple-junction cells are likely to be explained by assuming the electrical coupling among subcells.

ACKNOWLEDGEMENT

The authors are grateful to Drs. Ryusuke Onitsuka, Takaaki Agui, Hiroyuki Juso, and Tatsuya Takamoto of Sharp Corporation for their growth of InGaP/GaAs double-junction cell structures. This work was supported by the "Creative Research for Clean Energy Generation Using Solar Energy" project in the Core Research for Evolutional Science and Technology (CREST) program of Japan Science and Technology Agency (JST).

REFERENCES

- [1] M. Yamaguchi, T. Takamoto, K. Araki, N. E.-Daukes, "Multi-junction III-V solar cells: current status and future potential", *Solar Energy*, vol. 79, pp. 78-85, 2005.
- [2] J. F. Geisz, S. Kurtz, M. W. Wanlass, J. S. Ward, A. Duda, D. J. Friedman, J. M. Olson, W. E. McMahon, T. E. Moriarty, and J. T. Kiehl, "High-efficiency GaInP/GaAs/InGaAs triple-junction solar cells grown inverted with a metamorphic bottom junction", *Appl. Phys. Lett.* vol. 9, pp. 023502-1-023502-3, 2007.
- [3] F. Dimroth, et al. "Wafer bonded four-junction GaInP/GaAs/GaInAsP/GaInAs concentrator solar cells with 44.7% efficiency", *Prog. Photovolt: Res. Appl.* vol. 22, pp. 277-282 2014.
- [4] T. Soga, K. Baskar, T. Kato, T. Jimbo, and M. Umeno, "MOCVD growth of high efficiency current-matched AlGaAs/Si tandem solar cell", *J. Cryst. Growth*, vol. 174, pp. 579-584, 1997.
- [5] K. Tanabe, K. Watanabe, and Y. Arakawa, "III-V/Si hybrid photonic devices by direct fusion bonding", *Sci. Rep.* vol. 2, pp. 349-354, 2012.
- [6] K. Derendorf, et al. "Fabrication of GaInP/GaAs/Si solar cells by surface activated direct wafer bonding", *IEEE J. Photovoltaics*, vol. 3, no. 4, pp. 1423-1428, 2013.
- [7] H. Takagi, K. Kikuchi, R. Maeda, T. R. Chung, and T. Suga, "Surface activated bonding of silicon wafers at room temperature", *Appl. Phys. Lett.* vol. 68, pp. 2222-2224, 1996.
- [8] M. M. R. Howlader, T. Watanabe, and T. Suga, "Characterization of the bonding strength and interface current of p-Si/n-InP wafers bonded by surface activated bonding method at room temperature", *J. Appl. Phys.* vol. 91 pp. 3062-3066, 2002.
- [9] J. Liang, T. Miyazaki, M. Morimoto, S. Nishida, N. Watanabe, and N. Shigekawa, "Electrical properties of p-Si/n-GaAs heterojunctions by using surface-activated bonding", *Appl. Phys. Express*, vol. 6, pp. 021801-1-021801-3, 2013.
- [10] J. Liang, S. Nishida, M. Morimoto, and N. Shigekawa, "Surface-activating-bonding-based low-resistance Si/III-V junctions", *Elec. Lett.* vol. 49 pp. 830-832, 2013.
- [11] N. Shigekawa, M. Morimoto, S. Nishida, and J. Liang, "Surface-activated-bonding-based InGaP-on-Si double-junction cells", *Jpn. J. Appl. Phys.* vol. 53, pp. 04ER05-1-04ER05-4, 2014.
- [12] N. Shigekawa, L. Chai, M. Morimoto, J. Liang, R. Onitsuka, T. Agui, H. Juso, and T. Takamoto, "Hybrid triple-junction solar cells by surface activated bonding of III-V double-junction-cell heterostructures to ion-implantation-based Si cells", *Proc. 40th IEEE Photovoltaic Specialists Conference*, pp. 534-537 (2014).
- [13] N. Shigekawa, J. Liang, R. Onitsuka, T. Agui, H. Juso, and T. Takamoto, "Current-voltage and spectral-response characteristics of surface-activated-bonding based InGaP/GaAs/Si hybrid triple-junction cells", *accepted for publication in Jpn. J. Appl. Phys.*
- [14] N. Chand, P. A. Houston, and P. N. Robson, *IEEE Trans. Electron Devices*, **ED-32** 622 (1985). "Gain of a heterojunction bipolar photo-transistor", *IEEE Tran. Electron Devices* vol. ED-32, no. 3, pp. 622-627 (1985).
- [15] T. Suemitsu, H. Fushimi, S. Kodama, S. Tsunashima, and S. Kimura, "Influence of hole accumulation on source resistance, kink effect and on-state breakdown of InP-based high electron mobility transistors: light irradiation study", *Jpn. J. Appl. Phys.* vol. 41, no. 2B, pp. 1104-1107 (2002).